

## Target Detection in Compound-Gaussian Clutter with Adaptive OFDM Radar

Yang Xia<sup>\*</sup>, Zhiyong Song, Zaiqi Lu, and Qiang Fu

**Abstract**—This paper mainly deals with the problem of target detection in compound-Gaussian clutter with orthogonal frequency division multiplexing (OFDM) radar. First, the OFDM measurement model is developed to compound-Gaussian clutter by taking advantage of frequency diversity of OFDM radar waveform and we devise a generalized likelihood ratio test (GLRT) detector where the target scattering coefficients and clutter covariance matrix are unknown. Then, we propose an adaptive waveform design scheme based on maximizing Mahalanobis distance of the distributions under two hypotheses to improve the detection performance. Finally, the effectiveness of the proposed detector as well as the adaptive waveform design method is demonstrated via numerical examples.

### 1. INTRODUCTION

Orthogonal frequency division multiplexing (OFDM) was originally proposed as a digital modulation technique in communication fields and later on introduced into radar community [1, 2]. The first investigations on the suitability of multicarrier waveforms for radar applications were published in 2000 by Levanon [3]. As a new broadband radar signal, OFDM has drawn much attention due to the flexibly available spectral resources, good ambiguity function (AF) and frequency diversity characteristic [4, 5]. The frequency diversity provides additional information that enhances targets detection from background clutter, especially in multipath scenarios [6]. A large amount of research works have been done on OFDM radar such as target detection and tracking [7], direction of arrival (DOA) estimation [8] and synthetic aperture radar (SAR) imaging [9], etc.

The target detection problem with OFDM radar has attracted considerable attention recently. Focusing on the issue of moving target detection in the presence of multipath reflections, an optimized detection algorithm with OFDM radar was proposed in [10], where the spatial and frequency diversities are exploited. The problem of target detection in multipath scenarios is reformulated as sparse spectrum estimation and the spectral parameters of OFDM radar waveform are optimized based on multi-objective optimization (MOO) technique to improve the detection performance [11]. The performances of generalized likelihood ratio test (GLRT) detector with OFDM radar in non-Gaussian clutter (including Log-normal, Weibull and K-compound distribution) were investigated in [12, 13] and target fluctuations were also taken into consideration.

In real clutter environments, the distribution of clutter usually deviates from the Gaussian assumption especially in high-resolution radar or low grazing angle scenario. Instead, a compound-Gaussian model is adopted which is the product of a temporally slow-changing texture component and a locally fast-changing speckle component [14].

In this paper, we address the problem of target detection in compound-Gaussian clutter with OFDM radar. Since the target scattering coefficients and clutter covariance are unknown, a GLRT detector is developed where the unknown parameters are replaced with their maximum likelihood estimates (MLEs). Based on maximizing Mahalanobis distance of the distributions under two hypotheses, an

---

*Received 20 October 2015, Accepted 11 December 2015, Scheduled 19 December 2015*

<sup>\*</sup> Corresponding author: Yang Xia (xiayang@nudt.edu.cn).

The authors are with the ATR Key Laboratory, National University of Defense Technology, Changsha 410073, P. R. China.

adaptive waveform design method is proposed to improve the detection performance. Several numerical examples are provided to evaluate performance of the proposed detector and the adaptive waveform design method.

## 2. PROBLEM FORMULATION

### 2.1. Measurement Model

We consider a monostatic radar employing an OFDM signaling system, which simultaneously transmits  $N$  subcarriers. The time duration of a single pulse is  $t_b$  and the subcarrier spacing is  $\Delta f$ . To keep orthogonal between different subcarriers,  $\Delta f$  is the reciprocal of  $t_b$ . The complex envelop of a single pulse can be represented as

$$s(t) = \sum_{n=0}^{N-1} w_n e^{j2\pi(f_0+n\Delta f)t}, \quad 0 \leq t \leq t_b \quad (1)$$

where  $f_0$  is the carrier frequency and  $\mathbf{w} = [w_0, w_1, \dots, w_{N-1}]^T$  represent the complex weights transmitted over different subcarriers and satisfying  $\sum_{n=0}^{N-1} |w_n|^2 = 1$ . The total bandwidth is  $B = N\Delta f$ .

Considering a moving target with relative velocity  $\mathbf{v}$  at a distance  $R$  from the radar, the geometry of this scenario is shown in Figure 1. The received signal corresponding to the  $n$ -th subchannel can be written as

$$y_n(t) = s_n(\gamma(t - \tau)) + c_n(t) \quad (2)$$

where  $\gamma = 1 + \beta$  represents the stretching or compressing in time of the reflected signal, and  $\beta = 2\langle \mathbf{v}, \mathbf{u} \rangle / c$  is the Doppler spreading factor.  $\mathbf{u}$  and  $c$  denote the unit direction of arrival (DOA) vector and the propagation speed, respectively;  $\tau$  is the roundtrip delay;  $c_n(t)$  represents the background clutter corresponding to the  $n$ -th subchannel. Substituting (1) into (2) yields

$$y_n(t) = w_n x_n e^{-j2\pi f_n \gamma \tau} e^{j2\pi f_n \beta t} + c_n(t) \quad (3)$$

where  $f_n = f_0 + n\Delta f$  and  $x_n$  denotes the target scattering coefficient corresponding to the  $n$ -th subcarrier. We incorporate information of the known range cell (denoted by the roundtrip delay  $\tau$ ) by substituting  $t = \tau + mT_r$  ( $m = 0, 1, \dots, M-1$ ), where  $T_r$  and  $M$  denote the pulse repetition interval (PRI) and pulse number within one coherent processing interval (CPI) respectively. Hence, the received signal can be written as

$$y_n(m) = w_n x_n \phi_n(m) + c_n(m) \quad (4)$$

where

$$\phi_n(m) = e^{-j2\pi f_n \tau} e^{j2\pi f_n \beta m T_r} \quad (5)$$

Stacking the measurements of all subchannels into an  $N \times 1$  vector, we get

$$\mathbf{y}(m) = \mathbf{W}\Phi(m)\mathbf{x} + \mathbf{c}(m) \quad (6)$$

where

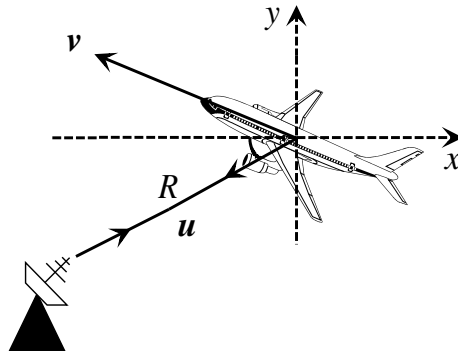


**Figure 1.** Schematic representation of moving target detection scenario.

- $\mathbf{y}(m) = [y_0(m), y_1(m), \dots, y_{N-1}(m)]^T$ .
- $\mathbf{W} = \text{diag}(w_0, w_1, \dots, w_{N-1})$  is an  $N \times N$  complex diagonal matrix that represents the transmitted weights.
- $\mathbf{\Phi}(m) = \text{diag}(\phi_0(m), \phi_1(m), \dots, \phi_{N-1}(m))$  is an  $N \times N$  diagonal matrix that contains Doppler information of the target.
- $\mathbf{c}(m) = [c_0(m), c_1(m), \dots, c_{N-1}(m)]^T$  is an  $N \times 1$  vector of clutter returns.

Then concatenating all the temporal data into an  $NM \times 1$  vector, we obtain

$$\mathbf{y} = \mathbf{\Phi}\mathbf{x} + \mathbf{c} \quad (7)$$

where

- $\mathbf{y} = [\mathbf{y}(0)^T, \mathbf{y}(1)^T, \dots, \mathbf{y}(M-1)^T]^T$ .
- $\mathbf{\Phi} = [\mathbf{W}\mathbf{\Phi}(0), \mathbf{W}\mathbf{\Phi}(1), \dots, \mathbf{W}\mathbf{\Phi}(M-1)]^T$  is an  $NM \times N$  matrix containing the target Doppler information over different pulses.
- $\mathbf{c} = [\mathbf{c}(0)^T, \mathbf{c}(1)^T, \dots, \mathbf{c}(M-1)^T]^T$  is an  $NM \times 1$  vector comprising the clutter returns.

## 2.2. Statistical Model

In this paper, the clutter is modeled as compound-Gaussian distribution which is the product of texture and speckle component. The texture is assumed to vary from pulse to pulse while the speckle changes between different subchannels. More specifically, the clutter is modeled as [15]

$$\mathbf{c}(m) = \sqrt{u_m} \mathbf{g}_m, \quad m = 0, 1, \dots, M-1 \quad (8)$$

where  $\{u_m\}_{m=0}^{M-1}$  are nonnegative real random process and  $\{\mathbf{g}_m\}_{m=0}^{M-1}$  are complex Gaussian vectors with known covariance matrix  $\mathbf{\Sigma}$ . Thus  $\mathbf{c}$  is the compound-Gaussian random vector with unknown covariance matrix

$$\mathbf{R} = E[\mathbf{c}\mathbf{c}^H] = \mathbf{U} \otimes \mathbf{\Sigma} \quad (9)$$

where  $\mathbf{U} = \text{diag}(u_0, u_1, \dots, u_{M-1})$  which is considered as a deterministic matrix with unknown parameters  $\{u_0, u_1, \dots, u_{M-1}\}$ .  $\otimes$  and  $E[\cdot]$  denotes Kronecker product and the statistical expectation, respectively.

## 3. DETECTOR DESIGN

In this section, we develop a statistic detection test for the OFDM measurement model in Section 2. The essence of detection is to judge whether a target is present or not in the range cell under test. This is a classical two-hypothesis detection problem. So, we construct a decision problem to choose between two possible hypotheses: the null hypothesis (target-free hypothesis) and the alternate hypothesis (target-present hypothesis), which can be expressed as

$$\begin{cases} \mathcal{H}_0 : \mathbf{y} = \mathbf{c} \\ \mathcal{H}_1 : \mathbf{y} = \mathbf{\Phi}\mathbf{x} + \mathbf{c} \end{cases} \quad (10)$$

In this typical two-hypothesis detection problem, Neyman-Pearson (NP) detector is the optimal detector which maximizes the probability of detection at a constant probability of false alarm. However,  $\mathbf{x}$  and  $\mathbf{U}$  are unknown in our problem. Therefore, a GLRT detector is adopted and the unknown parameters are replaced with their MLEs. The detection problem can be denoted as the following decision

$$\frac{\max_{\mathbf{x}, \mathbf{v}, u_0, \dots, u_{M-1}} f(\mathbf{y} | \mathcal{H}_1, \mathbf{x}, \mathbf{v}, u_0, \dots, u_{M-1})}{\max_{u_0, \dots, u_{M-1}} f(\mathbf{y} | \mathcal{H}_0, u_0, \dots, u_{M-1})} \underset{\mathcal{H}_0}{\overset{\mathcal{H}_1}{\gtrless}} \gamma \quad (11)$$

where

- $\gamma$  is the detection threshold which is dependent on the false alarm rate.

- $f(\mathbf{y}|\mathcal{H}_0, u_0, \dots, u_{M-1})$  denotes the probability density function (PDF) under  $\mathcal{H}_0$  hypothesis, which is

$$f(\mathbf{y}|\mathcal{H}_0, u_0, \dots, u_{M-1}) = \frac{1}{\pi^{NM} \det(\mathbf{R})} \exp\{-\mathbf{y}^H \mathbf{R}^{-1} \mathbf{y}\} \quad (12)$$

- $f(\mathbf{y}|\mathcal{H}_1, u_0, \dots, u_{M-1}, \mathbf{x})$  denotes the PDF under  $\mathcal{H}_1$  hypothesis, which is

$$f(\mathbf{y}|\mathcal{H}_1, u_0, \dots, u_{M-1}, \mathbf{x}) = \frac{1}{\pi^{NM} \det(\mathbf{R})} \exp\{-(\mathbf{y} - \Phi \mathbf{x})^H \mathbf{R}^{-1} (\mathbf{y} - \Phi \mathbf{x})\} \quad (13)$$

To determine the MLEs of  $\{u_0, u_1, \dots, u_{M-1}\}$ , the log-likelihood function of (12) is

$$\ln f(\mathbf{y}|\mathcal{H}_0, u_0, \dots, u_{M-1}) = -MN \ln \pi - M \ln \det(\Sigma) - N \sum_{m=0}^{M-1} u_m - \sum_{m=0}^{M-1} \frac{\mathbf{y}^H (\mathbf{E}_{mm} \otimes \Sigma^{-1}) \mathbf{y}}{u_m} \quad (14)$$

where  $\mathbf{E}_{mm}$  denotes the elementary matrix with component  $e(m, m) = 1$  for  $m = 0, 1, \dots, M-1$  and zeros for others.

Taking derivatives of (14) with respect to  $u_m$  and making it equal to zero, we get the MLE of  $u_m$  under  $\mathcal{H}_0$

$$\hat{u}_m = \frac{\mathbf{y}^H (\mathbf{E}_{mm} \otimes \Sigma^{-1}) \mathbf{y}}{N} \quad (15)$$

Similarly, the log-likelihood function of (13) is

$$\begin{aligned} \ln f(\mathbf{y}|\mathcal{H}_1, u_0, \dots, u_{M-1}, \mathbf{x}) &= -MN \ln \pi - M \ln \det(\Sigma) \\ &\quad - N \sum_{m=0}^{M-1} u_m - \sum_{m=0}^{M-1} \frac{(\mathbf{y} - \Phi \mathbf{x})^H (\mathbf{E}_{mm} \otimes \Sigma^{-1}) (\mathbf{y} - \Phi \mathbf{x})}{u_m} \end{aligned} \quad (16)$$

Taking derivatives of (16) with respect to  $u_m$  and making it equal to zero, we get the MLE of  $u_m$  under  $\mathcal{H}_1$

$$\hat{u}_m = \frac{(\mathbf{y} - \Phi \mathbf{x})^H (\mathbf{E}_{mm} \otimes \Sigma^{-1}) (\mathbf{y} - \Phi \mathbf{x})}{N} \quad (17)$$

The MLE of  $\mathbf{x}$  can be obtained via

$$\arg \min_{\mathbf{x}} \{(\mathbf{y} - \Phi \mathbf{x})^H \mathbf{R}^{-1} (\mathbf{y} - \Phi \mathbf{x})\} \quad (18)$$

The solution of (18) is [16]

$$\hat{\mathbf{x}} = (\Phi^H \mathbf{R}^{-1} \Phi)^{-1} \Phi^H \mathbf{R}^{-1} \mathbf{y} \quad (19)$$

From (17) and (19) we know that  $\{u_m\}_{m=0}^{M-1}$  and  $\mathbf{x}$  do not yield close-form MLE expressions. The usual way to circumvent this drawback is the cyclic maximisation method, which alternately search for the solution until convergence (see [17] for more details).

Finally, substituting  $\hat{u}_m$ ,  $\hat{\mathbf{x}}$  under  $\mathcal{H}_1$  and  $\mathcal{H}_0$  into (11)–(13), we come up with the following decision rule

$$\prod_{m=0}^{M-1} \frac{\mathbf{y}^H (\mathbf{E}_{mm} \otimes \Sigma^{-1}) \mathbf{y}}{(\mathbf{y} - \Phi \mathbf{x})^H (\mathbf{E}_{mm} \otimes \Sigma^{-1}) (\mathbf{y} - \Phi \mathbf{x})} \stackrel{\mathcal{H}_1}{\underset{\mathcal{H}_0}{\leq}} \gamma \quad (20)$$

#### 4. ADAPTIVE WAVEFORM DESIGN

In this section, we derive an adaptive waveform design method based on maximizing Mahalanobis distance of the distributions under two hypotheses to improve the detection performance. Since target scattering coefficients vary at different subcarriers, we can change the transmitted weights accordingly. The OFDM measurements under two possible hypotheses are distributed as

$$\begin{cases} \mathcal{H}_0 : \mathbf{y} \sim \mathcal{CN}_{NM}(\mathbf{0}, \mathbf{U} \otimes \Sigma) \\ \mathcal{H}_1 : \mathbf{y} \sim \mathcal{CN}_{NM}(\Phi \mathbf{x}, \mathbf{U} \otimes \Sigma) \end{cases} \quad (21)$$

Mahalanobis distance is a useful tool in multivariate statistical analysis and can be thought as a metric to measure the similarity between two distributions. It has been widely applied in outlier detection, data mining, cluster analysis and classification, etc. Besides Mahalanobis distance, there are also some other distance measures to evaluate the similarity, such as Bhattacharyya distance, Hellinger distance and Kullback-Leibler divergence, etc. However, these measures are defined in terms of integrals over the distributions and very few are available in closed form.

In our problem, the measurements under two hypotheses are distributed as complex multivariate normal distribution with the same covariance but different mean values. A standard measure to evaluate the similarity of two multivariate normal distributions is Mahalanobis distance [18]. Compared with other distance measures, Mahalanobis distance is more suitable in our problem considering its low computational complexity. Thus, we choose Mahalanobis distance as the distance measure. It is known that the larger the Mahalanobis-distance, the further the two distributions are separated and the better the detection performance [11, 19]. The squared Mahalanobis distance is defined as [20]

$$d^2 = (\Phi \mathbf{x})^H (\mathbf{U} \otimes \Sigma)^{-1} (\Phi \mathbf{x}) \quad (22)$$

Since  $\mathbf{U} = \text{diag}\{u_0, u_1, \dots, u_{M-1}\}$  and  $\Phi = [\mathbf{W}\Phi(0), \mathbf{W}\Phi(1), \dots, \mathbf{W}\Phi(M-1)]^T$ , Equation (22) can be reformulated as

$$d^2 = \sum_{m=0}^{M-1} u_m \mathbf{x}^H \Phi(m)^H \mathbf{W}^H \Sigma^{-1} \mathbf{W} \Phi(m) \mathbf{x} \quad (23)$$

and

$$\begin{aligned} \mathbf{x}^H \Phi(m)^H \mathbf{W}^H \Sigma^{-1} \mathbf{W} \Phi(m) \mathbf{x} &= \text{tr} \{ \mathbf{x}^H \Phi(m)^H \mathbf{W}^H \Sigma^{-1} \mathbf{W} \Phi(m) \mathbf{x} \} \\ &= \text{tr} \{ \Sigma^{-1} \mathbf{W} \Phi(m) \mathbf{x} \mathbf{x}^H \Phi(m)^H \mathbf{W}^H \} \end{aligned} \quad (24)$$

According to the theorem in [9], we have

$$\text{tr} \{ \Sigma^{-1} \mathbf{W} \Phi(m) \mathbf{x} \mathbf{x}^H \Phi(m)^H \mathbf{W}^H \} = \mathbf{w}^H [(\Phi(m) \mathbf{x} \mathbf{x}^H \Phi(m)^H)^T \odot \Sigma^{-1}] \mathbf{w} \quad (25)$$

where  $\odot$  denotes Hadamard product. Finally, the optimization problem can be represented as

$$\mathbf{w}_{\text{opt}} = \arg \max_{\mathbf{w} \in \mathbf{C}^N} \left\{ \mathbf{w}^H \left[ \sum_{m=0}^{M-1} u_m (\Phi(m) \mathbf{x} \mathbf{x}^H \Phi(m)^H)^T \odot \Sigma^{-1} \right] \mathbf{w} \right\} \quad \text{subject to } \mathbf{w}^H \mathbf{w} = 1 \quad (26)$$

In (26),  $\mathbf{w}^H \mathbf{w} = 1$  is the energy constraint and the above problem is the well-known Rayleigh quotient [21]. Thus, the solution of (26) is the eigenvector corresponding to the largest eigenvalue of  $[\sum_{m=0}^{M-1} u_m (\Phi(m) \mathbf{x} \mathbf{x}^H \Phi(m)^H)^T \odot \Sigma^{-1}]$ . First, a non-optimal  $\mathbf{w}$  will be transmitted in the first  $M$  pulses and then substituting the MLEs of  $\hat{\mathbf{x}}$  and  $\{\hat{u}_m\}_{m=0}^{M-1}$  into (26), the optimal transmit weights  $\mathbf{w}_{\text{opt}}$  are obtained and transmitted in the next  $M$  pulses.

## 5. NUMERICAL RESULTS

In this section, we present several numerical examples to illustrate performances of the proposed GLRT detector. Since the close-form expression for detection probability ( $P_d$ ) and false alarm rate ( $P_{fa}$ ) are difficult to obtain, we resort to Monte Carlo (MC) method which is based on  $100/P_{fa}$  independent trials.

We assume that the compound-Gaussian clutter is distributed as  $K$  distribution, whose PDF is

$$f(z) = \frac{\sqrt{2v/\mu}}{\Gamma(v)} \left( \sqrt{\frac{2v}{\mu}} z \right)^v K_{v-1} \left( \sqrt{\frac{2v}{\mu}} z \right) \quad (27)$$

and the texture component follows a gamma distribution with PDF

$$f(s) = \frac{1}{\Gamma(v)} \left( \frac{v}{\mu} \right)^v s^{v-1} e^{-v/\mu s} \kappa(s) \quad (28)$$

where  $\Gamma(\cdot)$  is Eulerian Gamma function,  $\kappa(\cdot)$  is unit step function and  $K_{v-1}(\cdot)$  is the modified Bessel function of second kind with order  $v - 1$ .  $\mu$  and  $v$  are the scale and shape parameter, respectively. Noting that  $v$  is related to the spikiness of clutter, the smaller the value of  $v$ , the spikier the clutter. If  $v \rightarrow \infty$ , the  $K$  distribution will become Gaussian.

Additionally, the speckle component is assumed to be Gaussian distribution with exponential correlation structure covariance matrix [22]

$$[\Sigma]_{i,j} = \rho^{|i-j|}, \quad \text{for } i, j = 0, 1, \dots, N - 1 \quad (29)$$

where  $\rho$  is one-lag correlation coefficient. The signal-to-clutter ratio (SCR) is defined as

$$\text{SCR} = \frac{1}{M} \frac{(\Phi \mathbf{x})^H (\Phi \mathbf{x})}{E\{\tau\} \text{tr}(\Sigma)} \quad (30)$$

and the simulation parameters are shown in Table 1.

In the simulation, we choose different subcarriers ( $N = 1, 3, 5$ ) to demonstrate the influence of frequency diversity on the detection performance. Though we select only a small number of subcarriers in the simulation, our method is applicable to a larger number of subcarriers (we have not specified the value of  $N$  in the derivation). From Equation (7) we can see that dimension of the measurement is  $NM \times 1$ . As the number of subcarrier increases, the dimension of measurement will grow rapidly and it

**Table 1.** Parameter settings of the simulations.

Parameters	Values	Parameters	Values
Speed of light $c$	$3 \times 10^8$ m/s	Bandwidth $B$	100 MHz
Velocity of target	20 m/s	Carrier numbers $N$	1, 3, 5
Target moving direction	random	Frequency weights $\mathbf{W}$	$1/\sqrt{N} \mathbf{I}_N$
Scattering coefficient matrix of target $\mathbf{x}$	$\mathcal{CN}(0, 1)$	Pulse number $M$	16
Height of radar platform	100 m	Pulse repetition interval $T_r$	2 ms
Velocity of radar platform	$[0 \ 0]^T$ m/s	False alarm rate $P_{fa}$	$10^{-3}$
Relative distance between radar and target	5 km	One-lag correlation coefficient $\rho$	0.9
Height of target	200 m	Scale parameter of clutter $\mu$	1
Carrier frequency $f_0$	1 GHz	Shape parameter of clutter $v$	0.5, 1, 100

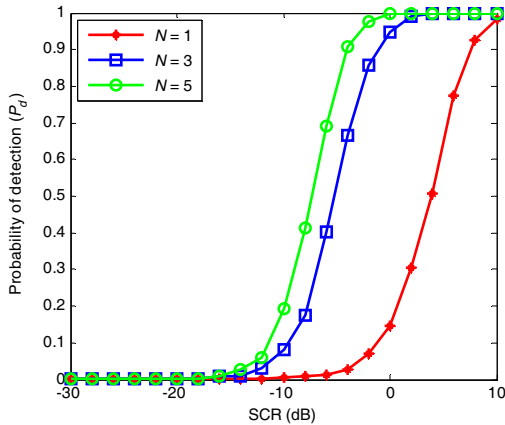


**Figure 2.** Effect of the carrier number on the detection performance.

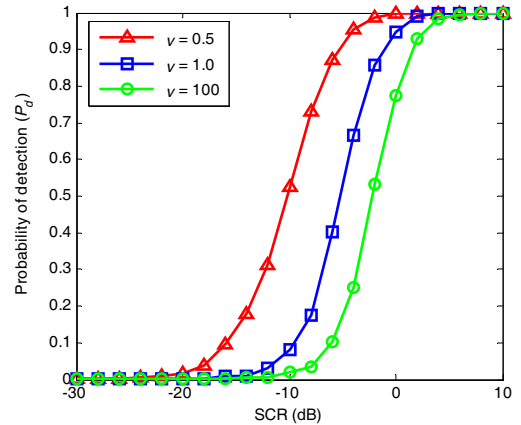


**Figure 3.** Effect of shape parameter on the detection performance.

would be difficult to compute. Hence we select a small number of subcarriers to evaluate our algorithm (in similar literatures, [10] sets  $N = 2, 4, 6$  and [13] sets  $N = 1, 3, 5$ ).

In Figure 2, we show the effect of carrier number on the detection performance, where  $P_d$  is plot against SCR with different carrier numbers. Parameters used in this simulation include  $v = 1$  and  $\rho = 0.9$ . The curves indicate that performance of the proposed detector is improved with increasing the number of subcarriers. Specifically, when  $P_d = 0.9$  the performance gap is about 13.4 dB between  $N = 1$  and  $N = 3$ , and about 3.3 dB between  $N = 3$  and  $N = 5$ . The results show that the frequency diversity improves the detection performance in an OFDM radar system.

Figure 3 shows the detection performance with different shape parameters, where  $N = 3$  and  $\rho = 0.9$ . The results show that performance of the GLRT detector is increased with decreasing value of  $v$ . For instance, the performance gap between  $v = 0.5$  and  $v = 100$  is about 6.9 dB when  $P_d = 0.9$ . This is because when  $v$  is large enough, the distribution of clutter approaches Gaussian and the detection performance will become worse due to the clutter model mismatch. In other words, the curves show that performance of the proposed detector is increased with spikier clutter.

In Figure 4, the effect of correlation coefficient  $\rho$  on the detection performance is investigated, where  $N = 3$  and  $v = 1$ . The results indicate that the performance is better with smaller correlation coefficient. For instance, the performance gap between  $\rho = 0.2$  and  $\rho = 0.9$  is 5.4 dB when  $P_d = 0.9$ . The results indicate the detection performance decreases with the increasing of correlation coefficient.

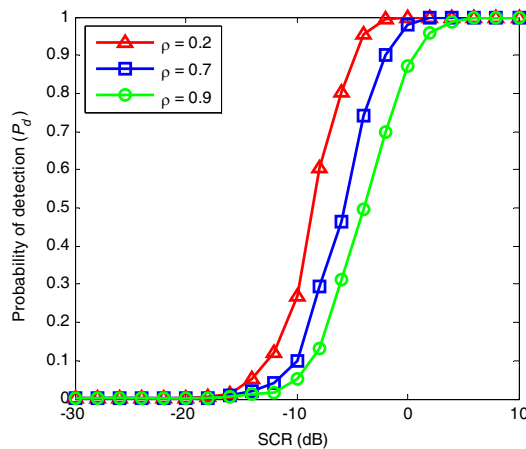


Figure 4. Effect of correlation coefficient on the detection performance.

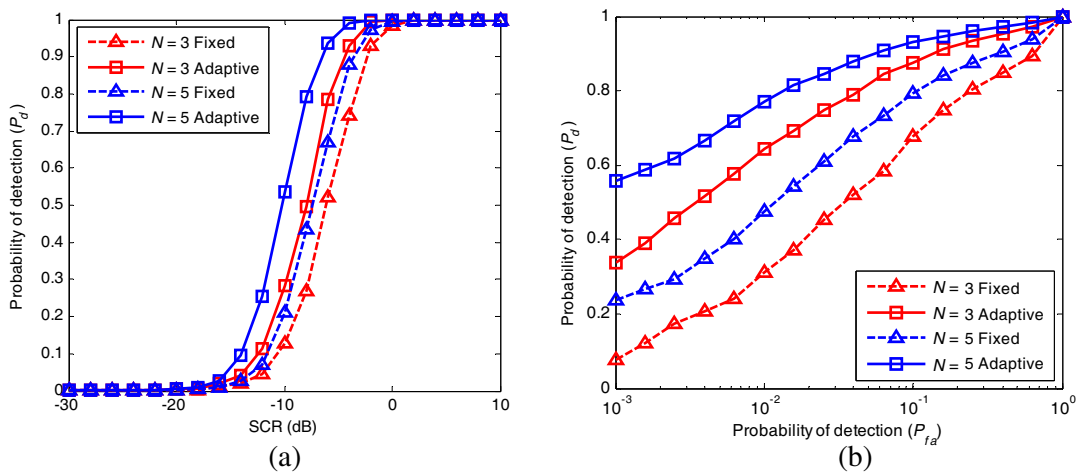


Figure 5. Detection performance comparison with fixed and adaptive waveform (a)  $P_d$  versus SCR when  $P_{fa} = 10^{-3}$ ; (b)  $P_d$  versus  $P_{fa}$  when SCR =  $-10$  dB.

Finally, in Figure 5 we show the detection performance improvement due to the adaptive waveform design. Parameters used in this simulation include  $N = 3, 5$ ,  $\rho = 0.9$  and  $v = 1$ . Figure 5(a) shows  $P_d$  versus SCR when  $P_{fa} = 10^{-3}$  while Figure 5(b) shows  $P_d$  versus  $P_{fa}$  when SCR = -10 dB. We assume that equal frequency weights are transmitted in the first  $M$  pulses, i.e.,  $\mathbf{w} = 1/\sqrt{N}\mathbf{I}$ . Then we compute the optimal values of  $\mathbf{w}$  through solving (26) for the next  $M$  pulses. The results demonstrate that compared with fixed waveform the detection performance is improved using adaptive waveform design method proposed in this paper.

## 6. CONCLUSIONS

In this paper, we developed a GLRT detector for an OFDM radar system in compound-Gaussian clutter when the target and clutter parameters are unknown. We derived an OFDM radar measurement model and formulated the detection problem as statistical hypothesis test, where the unknown parameters are estimated using cyclic maximisation method. We proposed a waveform design method which adaptively changed the transmitted weights based on Mahalanobis distance. We used MC simulations to demonstrate the advantage of frequency diversity of an OFDM radar system and detection performance improvement due to the adaptive waveform design.

## 7. DISCLOSURE STATEMENT

No potential conflict of interest was reported by the authors.

## ACKNOWLEDGMENT

This work was supported in part by the National Natural Science Foundation of China under No. 61401475.

## REFERENCES

1. Jankiraman, M., B. J. Wessels, and P. V. Genderen, "Design of a multi-frequency FMCW radar," *Proceedings of the 28th European Microwave Conference*, 548–589, Amsterdam, Netherlands, 1998.
2. Varzakas, P., "Optimization of an OFDM Rayleigh fading system," *International Journal of Communication Systems*, Vol. 20, No. 1, 1–7, 2007.
3. Levanon, N., "Multifrequency complementary phase-coded radar signal," *IEE Proc. Radar, Sonar and Navigation*, Vol. 147, No. 6, 276–284, 2000.
4. Mohseni, R., A. Sheikhi, and M. A. Masnadi-Shirazi, "Compression of multicarrier phase-coded radar signals based on discrete Fourier transform (DFT)," *Progress In Electromagnetics Research C*, Vol. 5, 93–117, 2008.
5. Kim, J. H., M. Younis, and W. Wiesbeck, "A novel OFDM chirp waveform scheme for use of multiple transmitters in SAR," *IEEE Geoscience and Remote Sensing Letters*, Vol. 10, No. 3, 568–572, 2013.
6. Sen, S. and A. Nehorai, "Target detection in clutter using adaptive OFDM radar," *IEEE Signal Processing Letters*, Vol. 16, No. 7, 592–598, 2009.
7. Sen, S. and A. Nehorai, "OFDM MIMO radar with mutual-Information waveform design for low-grazing angle tracking," *IEEE Transaction on Signal Processing*, Vol. 58, No. 6, 3152–3162, 2010.
8. Wu, X. H., A. A. Kishk, and A. W. Glisson, "MIMO-OFDM radar for direction estimation," *IET Radar, Sonar & Navigation*, Vol. 4, No. 1, 28–36, 2010.
9. Garmatyuk, D. and M. Brenneman, "Adaptive multicarrier OFDM SAR signal processing," *IEEE Transactions on Geoscience and Remote Sensing*, Vol. 49, No. 10, 3780–3790, 2011.
10. Sen, S. and A. Nehorai, "Adaptive OFDM radar for target detection in multipath scenarios," *IEEE Transaction on Signal Processing*, Vol. 59, No. 1, 78–90, 2011.

11. Sen, S., G. Tang, and A. Nehorai, "Multi-objective optimization of OFDM radar waveform for target detection," *IEEE Transaction on Signal Processing*, Vol. 59, No. 2, 639–652, 2011.
12. Kafshgari, S. and R. Mohseni, "The effect of target fluctuation on the OFDM radar detection performance," *Proceedings of 20th Telecommunications Forum (TELFOR)*, 827–830, Belgrade, 2012.
13. Kafshgari, S. and R. Mohseni, "Fluctuating target detection in presence of non Gaussian clutter in OFDM radars," *International Journal of Electronics and Communications (AEÜ)*, 885–893, 2013.
14. Conte, E. and M. Longo, "Modeling and simulation of non-Rayleigh radar clutter," *IEE Proc. — F Radar and Signal Processing*, Vol. 138, No. 2, 121–130, 1991.
15. Akcakaya, M. and A. Nehorai, "Adaptive MIMO radar design and detection in compound-Gaussian clutter," *IEEE Transactions on Aerospace and Electronic System*, Vol. 47, No. 3, 2200–2207, 2011.
16. Maio, A. D. and M. Lops, "Design principles of MIMO radar detectors," *IEEE Transactions on Aerospace and Electronic System*, Vol. 43, No. 3, 886–898, 2007.
17. Cui, G., L. Kong, and X. Yang, "Multiple-input multiple-output radar detectors design in non-Gaussian clutter," *IET Radar, Sonar & Navigation*, Vol. 4, No. 5, 724–732, 2010.
18. Mahalanobis, P. C., "On the generalized distance in statistics," *Proc. Nat. Inst. Sci. India*, Vol. 2, 49–55, 1936.
19. Anderson, T. W., *An Introduction to Multivariate Statistical Analysis*, 3rd Edition, Wiley, Hoboken, NJ, 2003.
20. Maesschalck, R. D., D. Jouan-Rimbaud, and D. L. Massart, "The Mahalanobis distance," *Chemometrics and Intelligent Laboratory Systems*, Vol. 50, 1–18, 2010.
21. Horn, R. A. and C. R. Johnson, *Matrix Analysis*, Cambridge Univ. Press, Cambridge, U.K., 1990.
22. Li, N., G. Cui, and L. Kong, "MIMO radar moving target detection against compound Gaussian clutter," *Circuits Syst. Signal Process*, Vol. 33, 1819–1839, 2014.